Polymer Chemistry

PAPER

View Article Online
View Journal | View Issue

Cite this: *Polym. Chem.*, 2018, **9**, 1735

The effects of polymer topology and chain length on the antimicrobial activity and hemocompatibility of amphiphilic ternary copolymers†

Rashin Namivandi-Zangeneh,[a] Rebecca J. Kwan,[a] Thuy-Khanh Nguyen,[a] Jonathan Yeow,[a] Frances L. Byrne,[b] Stefan H. Oehlers,[c,d] Edgar H. H. Wong *[a] and Cyrille Boyer *[a]

Investigation into the macromolecular structure–activity relationship of synthetic antimicrobial polymers has been gaining scientific interest due to the possibility of discovering new alternatives for combating the increase of multidrug resistance in bacteria. Recently, we reported the development of new antimicrobial polymers in the form of amphiphilic ternary copolymers that consist of low-fouling (oligoethylene glycol), cationic and hydrophobic side chains. The combination of these three main functional groups is crucial in endowing the polymers with high antimicrobial potency against Gram-negative pathogens and low cytotoxicity. Following on from our previous study, we herein present a systematic assessment on the effects of the polymer chain length and architecture (*i.e.*, random *vs.* block copolymers and linear *vs.* hyperbranched) on the antimicrobial activity and hemocompatibility of antimicrobial ternary copolymers. The polymer chain length in random copolymers slightly affects the antimicrobial activity where longer chains are marginally more bacteriostatic against *Pseudomonas aeruginosa* and *Escherichia coli*. In terms of hemocompatibility, polymers with shorter chains are more prone to hemagglutination. Interestingly, when the hydrophilic and hydrophobic segments are separated into diblock copolymers, the antimicrobial activity is lost, possibly due to the stable core–shell architecture. The hyperbranched structure which consists of 2-ethylhexyl groups as hydrophobic side-chains yields the best overall biological properties, having similar antimicrobial activity (MIC = 64 μg mL^{-1}) and >4-fold increase in HC_{50} compared to the linear random copolymers (HC_{50} > 10 000 μg mL^{-1}) with no hemagglutination. The hyperbranched polymers are also bactericidal and kill ≥99% and 90% of planktonic and biofilm *Pseudomonas aeruginosa*, respectively. This study thus highlights the importance of determining macromolecular structural aspects that govern the biological activity of antimicrobial polymers.

Received 26th June 2017,
Accepted 17th August 2017

DOI: 10.1039/c7py01069a

rsc.li/polymers

Introduction

The increase of multidrug resistance in bacteria is now regarded as one of the most pressing healthcare issues worldwide.[1–4] Recently, the World Health Organization (WHO) published a list of "priority pathogens" which indicates the most threatening bacteria to human health that urgently requires new antibiotic treatments.[5] At the top of this list are carbapenem-resistant strains of *Acinetobacter baumannii* and *Pseudomonas aeruginosa* – both of which are Gram-negative bacteria. While the discovery of a new antibiotic called teixobactin offers hope in overcoming infections caused by Gram-positive bacteria such as methicillin-resistant *Staphylococcus aureus* (MRSA),[6] the pipeline for the development of new antimicrobial agents that combat Gram-negative bacteria remains limited.[7]

Drawing inspiration from (naturally occurring) antimicrobial peptides (AMPs) and driven by the advances of controlled polymerization techniques,[8–13] synthetic polymers have emerged as promising antimicrobial candidates in combating Gram-negative bacteria over the last few years. By mimicking

[a]*Centre for Advanced Macromolecular Design (CAMD) and Australian Centre for NanoMedicine (ACN), School of Chemical Engineering, UNSW Australia, Sydney, NSW 2052, Australia. E-mail: edgar.wong@unsw.edu.au, cboyer@unsw.edu.au*
[b]*School of Biotechnology and Biomolecular Sciences, UNSW Australia, Sydney, NSW 2052, Australia*
[c]*Tuberculosis Research Program, Centenary Institute, Camperdown, NSW 2050, Australia*
[d]*Sydney Medical School, The University of Sydney, Newtown, NSW 2006, Australia*
†Electronic supplementary information (ESI) available: Additional ^{1}H NMR results and movies. See DOI: 10.1039/c7py01069a

the structural composition of AMPs which primarily consist of cationic and hydrophobic moieties, synthetic antimicrobial polymers can exert their bactericidal properties through physical membrane disruption of the bacteria cell wall (*e.g.*, the outer and/or inner membrane of Gram-negative bacteria).[14–33] Unlike conventional antibiotics which target intracellular targets (*e.g.*, inhibition of DNA/RNA synthesis or cell wall synthesis), this particular mechanism hinders resistance development in bacteria towards AMPs and mimics thereof.[34] In addition, by combining the synthetic versatility of controlled polymerization techniques, complex antimicrobial polymers with precise macromolecular topologies and functionalities have been generated, some of which display improved biological properties compared to traditional linear analogues.[35] For example, Lam *et al.* recently reported the development of antimicrobial star-shaped polypeptides that exhibited excellent bactericidal properties through a multi-modal mechanism (*e.g.*, extensive membrane pore formation and triggering of immune responses in mice model studies) against various Gram-negative bacteria, including colistin-resistant strains.[36] The architecture was suggested to be a key factor in endowing the star polymers with the multi-modal mechanism and outstanding antimicrobial activity.

Evidently, investigation into the structure–bioactivity relationship of antimicrobial polymers is crucial, as this will not only improve our understanding on the polymer–bacteria interaction but also aid in the development of more potent polymers. Besides focusing on the antimicrobial activity, the bio- or hemo-compatibility of a polymer is an equally important point to consider especially for potential applications in a clinical setting where the polymers are used in topical or intravenous formulations and medical device coating.[37] Given that the cationic groups in antimicrobial polymers may also interact with mammalian cells and induce cytotoxicity, various efforts have been made to reduce this non-specific interaction, for instance, *via* the use of different types of cationic groups (*e.g.*, primary *vs.* secondary amines)[20,38–40] or manipulation of the polymer architecture (*e.g.*, mixed micelles and miktoarm star polymers).[41–43] In addition, several groups have also prepared antibacterial polymer coatings and gels with low-fouling properties using zwitterionic or ethylene glycol-based monomers to minimize non-specific interactions with proteins.[44–46] Very recently, we described the synthesis of new antimicrobial polymers in the form of single-chain polymeric nanoparticles (SCPNs) that demonstrated good biocompatibility and efficacy against both planktonic and biofilm Gram-negative bacteria.[47] These SCPNs were in essence amphiphilic ternary copolymers, and we found that the judicious combination of oligoethylene glycol (OEG), cationic mimic of 2,4-diaminobutyric acid (Dab), and hydrophobic (2-ethylhexyl or 2-phenylethyl) groups was necessary to achieve optimum antimicrobial activity and biocompatibility.[47]

Herein, we report a detailed investigation of various other factors that affect the antimicrobial activity and hemocompatibility of amphiphilic ternary copolymers, including the influence of the polymer chain length and topology (*i.e.*, random *vs.* block copolymers, and linear *vs.* hyperbranched polymers). For this study, various polymers are made using reversible addition–fragmentation chain transfer (RAFT) polymerization[8,13] (Fig. 1), and their antimicrobial activity is assessed based on the minimum inhibitory concentration (MIC) values. The MIC is defined as the minimum compound concentration

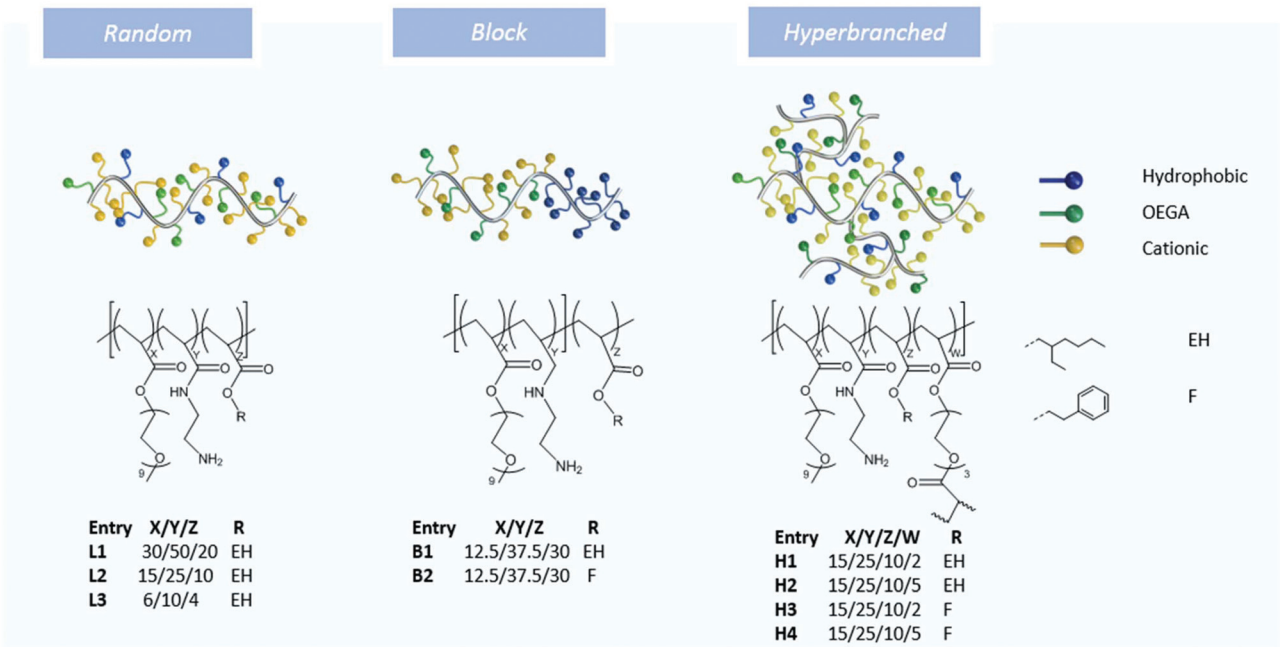

Fig. 1 The compositional structures and architectures of the amphiphilic ternary copolymers in this study.

that prevents visible bacterial growth. The most common method for determining the biocompatibility of antimicrobial polymers *in vitro* is by hemagglutination and hemolysis experiments where the HC_{50} value, defined as the compound concentration at which 50% of red blood cells are lysed, is used as a metric for comparison. Interestingly, polymers with different chain lengths (number-average degree of polymerization (DP_n) of 100, 50 and 20) have similar antimicrobial activities but different hemolytic activities. In addition, shorter polymer chains (DP_n = 50 and 20) cause hemagglutination. On the other hand, segregation of the hydrophilic OEG and cationic groups from hydrophobic moieties results in the loss of antimicrobial activity. Meanwhile, hyperbranched polymers indicate that branching can improve hemocompatibility (by >4 times) with only a minor loss of antimicrobial activity. Overall, this study yields valuable information pertaining to the structure–activity correlation of antimicrobial ternary copolymers.

Experimental section

Materials

Ethylenediamine (Sigma-Aldrich, ≥99%), di-*tert*-butyl dicarbonate (Aldrich, 99%), triethylamine (Scharlau, 99%), acryloyl chloride (Merck, ≥96%), 2-phenylethanol (Aldrich, ≥99%), oligoethylene glycol methyl ether acrylate (OEG acrylate) (M_n = 480 g mol^{-1}) (Aldrich), 2-ethylhexyl acrylate (Aldrich, 98%), oligoethylene glycol diacrylate (M_n = 250 g mol^{-1}) (Aldrich), trifluoroacetic acid (TFA) (Sigma-Aldrich, 99%), chloroform (VWR Chemicals), hexane (Merck), diethyl ether (Merck) and basic alumina (Al_2O_3) (LabChem) were used as received. 2,2′-Azobis (2-methylpropionitrile) (AIBN) (Acros, 98%) was purified by recrystallization from methanol. Sodium sulfate (Na_2SO_4), magnesium sulfate ($MgSO_4$), sodium hydrogen carbonate ($NaHCO_3$), tetrahydrofuran, and acetone were obtained from Chem-Supply and used as received. Milli-Q water with a resistivity of >18 MΩ cm was obtained from an in-line Millipore RiOs/Origin water purification system. The monomers *tert*-butyl (2-acrylamidoethyl) carbamate and 2-phenylethyl acrylate were synthesized according to literature procedures.[47]

Characterization of macromolecules

^{1}H nuclear magnetic resonance (NMR) spectra were recorded using a Bruker AC300F spectrometer. Deuterated solvents D_2O or $CDCl_3$ (obtained from Cambridge Isotope Laboratories) were used as reference solvents and samples with a concentration of *ca.* 10–20 mg mL^{-1} were prepared. The monomer composition in the polymers that consisted of 2-ethylhexyl acrylate was calculated using the following equation $\int a,b/6 : \int c/9 : \int d/2$ where $\int a, b, \int c,$ and $\int d$ correspond to the integrals of the characteristic protons of 2-ethylhexyl acrylate (methyl –CH_3– groups, δ_H 0.80–0.98 ppm), cationic monomer (*tert*-butyl –CH_3– groups, δ_H 1.38–1.52 ppm) and OEGA (ester –CH_2O– groups, 4.10–4.30 ppm), respectively (please refer to the ESI†). For polymers that consisted of 2-phenylethyl acrylate, the monomer composition was determined *via* the following equation $\int a,b/6 : \int c/9 : \int e/5$ where $\int e$ corresponds to the integrals of the characteristic protons of 2-phenylethyl acrylate (aromatic protons, δ_H 7.10–7.40 ppm).

Gel permeation chromatography (GPC) analysis was performed using a Shimadzu liquid chromatography system equipped with a Shimadzu refractive index detector and two MIX C columns (Polymer Lab) operating at 40 °C. Tetrahydrofuran was used as the eluent at a flow rate of 1 mL min^{-1}. The system was calibrated with poly(methyl methacrylate) standards with molecular weights of 200 to 10^6 g mol^{-1}.

Dynamic light scattering (DLS) and zeta-potential measurements were conducted using a Malvern Zetasizer Nano ZS apparatus equipped with a He–Ne laser operating at λ = 633 nm and at a scattering angle of 173°. All samples were prepared at a concentration of *ca.* 2 mg mL^{-1} where filtered Milli-Q water (using 0.45 μm pore size filter) was used as the solvent to solubilize the polymers.

Synthesis of linear random copolymers

The synthesis of linear random copolymers proceeded in the same manner as reported previously.[47]

Synthesis of block copolymers

To prepare the diblock copolymers, a macroRAFT agent was synthesized followed by chain extension with the hydrophobic monomers. Firstly, benzyl dodecyl carbonotrithioate (9.0 μmol), AIBN (4.5 μmol), OEGA (112.5 μmol) and *tert*-butyl (2-acrylamidoethyl) carbamate (337.5 μmol) were dissolved in 1,4-dioxane (such that the total monomer concentration was 1 M). The solution was degassed by bubbling with N_2 for 20 min and the reaction mixture was stirred at 70 °C for 3 h before cooling in an ice bath for 5 min. The polymer was purified by dialysis using a dialysis membrane (MWCO of 3.5 kDa) against methanol for 2 days, and was dried *in vacuo*. The macroRAFT agent was characterized by ^{1}H NMR and GPC analysis. For the chain extension step, the macroRAFT agent (4.5 μmol), hydrophobic monomer (135 μmol) and AIBN (2.25 μmol) were dissolved in 1,4-dioxane and the solution was degassed by bubbling with N_2 for 30 min in an ice bath. Then, the reaction mixture was stirred at 70 °C for 15 h. Polymerization was quenched by placing the flask in an ice bath for 5 min. The polymer was purified by precipitation into a diethyl ether/hexane (3 : 7) mixture. The precipitate was isolated by centrifugation, dissolved in methanol, and precipitated twice more. Finally, the polymer was dried *in vacuo*.

Synthesis of hyperbranched polymers

Hyperbranched polymers were synthesized in the same way as the linear random copolymers but with the addition of a cross-linkable monomer oligoethylene glycol diacrylate (M_n = 250 g mol^{-1}) at 2 and 5 molar equivalents with respect to the RAFT agent.

Removal of the Boc protecting groups

The Boc protecting groups were removed using TFA in the same manner as reported previously.[47]

Minimum inhibitory concentration (MIC) determination

The MIC was determined by using the broth microdilution method according to the Clinical and Laboratory Standards Institute (CLSI) guidelines. Briefly, bacterial culture was grown from a single colony in 10 mL of Mueller-Hinton broth (MHB) at 37 °C with shaking at 200 rpm overnight. The subculture was prepared from the overnight culture by diluting 1 : 100 in 5 mL MHB and allowed to grow to the mid-log phase, then diluted to the appropriate concentration for the MIC test. A two-fold dilution series of 50 μL of polymer solution in MHB were added into 96-well microplates followed by the addition of 50 μL of the subculture suspension. The final concentration of bacteria in each well was *ca.* 5×10^5 cells per mL. The plates were incubated at 37 °C for 20 h, and the absorbance at 600 nm was measured with a microtiter plate reader (FLUOstar Omega, BMG Labtech). MIC values were defined as the lowest concentration of the sample that showed no visible growth and inhibited cell growth by more than 90%. Positive controls without the polymer and negative controls without bacteria were included. All assays included two replicates and were repeated in at least three independent experiments.

Hemocompatibility studies

The hemolytic activity of the polymers was assessed using fresh sheep red blood cells (RBCs) obtained from Serum Australis (Catalog number SD50D). RBCs were diluted 1 : 20 in PBS (pH 7.4), pelleted by centrifugation and washed three times with PBS (1000*g*, 10 min). The RBCs were then resuspended to achieve 5% (v/v) in PBS. Different concentrations of polymers (150 μL) were prepared in sterilized tubes, followed by the addition of the RBC suspension (150 μL). The highest polymer concentration tested was 2 mg mL^{-1}. PBS buffer was used as a negative control while Triton-X 100 (1% v/v in PBS) was used as a positive hemolysis control. The tubes were incubated for 2 h at 37 °C and 150 rpm shaking speed in an incubator. Following incubation, the tubes were centrifuged (1000*g*, 8 min) and aliquots of the supernatants (100 μL) were transferred into a 96-well microplate where the absorbance values were monitored at 485 nm using a microtiter plate reader (FLUOstar Omega, BMG Labtech). The percentage of hemolysis was calculated using the absorbance values and the formula below:

$$\%\ \text{Hemolysis} = (A_{\text{polymer}} - A_{\text{negative}})/(A_{\text{positive}} - A_{\text{negative}}) \times 100\%$$

Bacteria killing studies

The laboratory strain *P. aeruginosa* PAO1 was used to investigate the bactericidal properties. Biofilms were grown as described in our previous study.[47] Briefly, in all assays, a single colony of PAO1 was inoculated in 10 mL of Luria Bertani medium (LB 10) at 37 °C with shaking at 200 rpm overnight. The overnight culture was diluted 1 : 100 in freshly prepared M9 minimal medium containing 48 mM Na_2HPO_4, 22 mM KH_2PO_4, 9 mM NaCl, 19 mM NH_4Cl, pH 7.0, supplemented with 2 mM $MgSO_4$, 100 μM $CaCl_2$ and 20 mM glucose. The bacterial suspension was then aliquoted using 1 mL per well of tissue-culture treated 24-well plates (Costar, Corning®). The plates were incubated at 37 °C with shaking at 180 rpm in an orbital shaker which does not stop agitation when the door is opened (model OM11, Ratek, Boronia, Australia) and the biofilm cultures were allowed to grow for 6.5 h without any disruption. The polymer was then added to the wells and the plates were incubated for 1 h. After treatment, the planktonic and biofilm viability analyses were determined by a drop plate method. For planktonic analysis, free-floating cells in the biofilm supernatant were serially diluted in sterile PBS and plated onto LB agar. For biofilm analysis, cells attached on the interior surfaces of the well (surface area 4.5 cm^2) were washed twice with sterile PBS to remove loosely attached bacteria, before being resuspended and homogenized in PBS by incubating in an ultrasonication bath (150 W, 40 kHz; Unisonics, Australia) for 20 min. Resuspended biofilm cells were then serially diluted and plated onto LB agar. Planktonic and biofilm colonies were counted and the CFU was calculated after 24 h incubation at 37 °C. All assays included two replicates and were repeated in at least three independent experiments.

Biofilm dispersal studies

To characterize the effect of the polymer on biofilm dispersal, preformed PAO1 biofilms were grown for 6.5 h and treated in the same manner as the killing study. Biofilm biomass was quantified by using the crystal violet (CV) staining method as previously described. Briefly, after treatment, the culture supernatant was removed and the biofilm on the well surfaces was washed once with 1 mL of PBS, followed by the addition of 1 mL 0.03% CV stain made from a 1 : 10 dilution of Gram crystal violet (BD) in PBS. The plates were incubated on the bench for 20 min before the wells were washed twice with PBS. The CV stained biofilms were mixed with 1 mL 100% ethanol and quantified by measuring the OD_{550} of the homogenized suspension using a microtiter plate reader (FLUOstar Omega, BMG Labtech). All assays included two replicates and were repeated in at least three independent experiments.

Biofilm imaging

To visualize the effect of the polymer on the biofilm, PAO1 biofilms were grown on 35 mm tissue culture dishes (FluoroDish, World Precision Instruments Inc., Sarasota, FL, USA) in the same way as in the bacteria killing study. The polymer was then added to the well and incubated for 1 h. After treatment, the supernatant was removed and the biofilm on the well surface was washed twice with 2 mL of PBS, followed by the addition of 1 mL PBS. The wells were analysed with a 3D tomographic microscope (3D Cell Explorer, NanoLive, Lausanne, Switzerland) equipped with a digital staining software. All assays were repeated in at least two independent experiments.

Results and discussion

In our previous report, we found that the combination of OEG, primary amine and hydrophobic groups in a single polymer

chain, where the functionalities were randomly distributed, was necessary to achieve optimal antimicrobial activity and biocompatibility.[47] Specifically, the low-fouling OEG was essential in preventing the formation of polymer–protein complexes which would hinder the antimicrobial efficacy. In addition, primary amine groups that mimic the amino acid, 2,4-diaminobutyric acid (Dab), yield better biocompatibility than amines that mimic lysine because of the shorter alkyl spacer group from the polymer backbone (2 *vs.* 4 $-CH_2-$). Furthermore, the incorporation of either 2-ethylhexyl or 2-phenylethyl groups as the hydrophobic component resulted in polymers that effectively cause bacterial membrane wall disruption with minimal resistance development, while maintaining relatively good cytocompatibility with mammalian cells. In theory, besides variation of the chemical composition, other factors such as the polymer chain length and topology could influence the biological properties of an antimicrobial polymer. Therefore, this study investigates the effect of various macromolecular structural variables on the biological properties of amphiphilic ternary copolymers. Each of these variables is chosen for specific reasons. Firstly, shorter polymer chain lengths (DP_n of 50 and 20 compared to 100 in our previous publication) are investigated as they mimic the length of most naturally occurring AMPs (20–40 amino acid residues per peptide chain).[34,48] Secondly, the block copolymer topology is examined as this architecture resembles the amphipathic characteristic of some AMPs (*e.g.*, melittin). Finally, branched architectures are evaluated since other similar examples (*e.g.*, star polymers[36,41]) have demonstrated improved bioactivity compared to the linear analogues. Like in our previous report, all ternary copolymers are synthesized *via* the RAFT polymerization[12] of OEG acrylate, *tert*-butyl (4-acrylamidobutyl) carbamate, and 2-ethylhexyl acrylate (or 2-phenylethyl acrylate) monomers, followed by the removal of *tert*-butyloxycarbonyl (Boc) protecting groups with TFA to yield primary amino groups.

Polymer chain length

Three linear random copolymers with DP_n of 100, 50 and 20 (denoted as L1, L2 and L3, respectively) that consist of 2-ethylhexyl groups as the hydrophobic component were synthesized to evaluate the effect of the polymer chain length on the antimicrobial activity and hemocompatibility. The molar feed ratio of OEG : amine : hydrophobic groups was fixed to 3 : 5 : 2 in all three polymers. The Boc-protected polymers produced monomodal molecular weight distributions with dispersity ($Đ$) values of *ca.* 1.2–1.4 as evidenced by GPC analysis (Fig. 2a and Table 1). It is noteworthy that the number-average molecular weight (M_n) values based on GPC analysis were relative to poly(methyl methacrylate) calibration standards and as such serve only as estimates. ^{1}H NMR analysis using the RAFT terminal groups as a reference showed good agreement with experimental and theoretical M_n values. Further analysis of the NMR spectra also confirmed the chemical compositions of the polymers to be identical to the molar feed ratio. The treatment of the polymers with TFA resulted in the quantitative removal of Boc groups, as confirmed by the absence of *tert*-butyl protons at δ_H 1.45 ppm (Fig. S1–S3, ESI†). The hydrodynamic diameter (D_h) of the Boc-deprotected polymers in water was determined by DLS measurements. Polymers L1, L2 and L3 have estimated D_h values of 0.8, 1.4 and 1.3 nm, respectively (Fig. 2b), which support the formation of single-chain polymeric nanoparticles in accord with our previous publication.[47] In addition, zeta potential (ζ) analysis of the polymers revealed that the polymers expectedly have net positive charges (+18.7 to +32.8 mV) due to the presence of primary amine groups.

The antimicrobial activity of the polymers was assessed *in vitro* against Gram-negative bacteria *Pseudomonas aeruginosa*

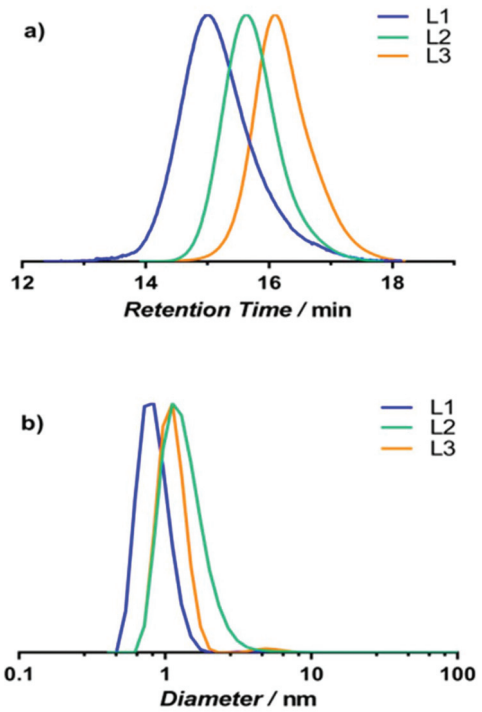

Fig. 2 (a) GPC-differential refractive index (DRI) chromatograms of the Boc-protected polymers L1, L2 and L3. (b) DLS normalized volume distributions of Boc-deprotected L1, L2 and L3 polymers in water.

Table 1 Polymer characterization by NMR, GPC, DLS and zeta potential analysis

Entry	M_n [a,b] (g mol^{-1})	M_n [b,c] (g mol^{-1})	$Đ$ [b,c]	D_h [d] (nm)	ζ [d] (mV)
L1	29 000	12 200	1.4	0.8	18.7
L2	14 800	8100	1.2	1.4	24.9
L3	6100	5000	1.2	1.3	32.8
B1	19 000	11 000	1.7	43.7	36.3
B2	18 300	10 500	1.5	24.6	28.6
H1	—	12 900	1.3	1.7	42.5
H2	—	17 200	1.6	1.6	36.1
H3	—	12 700	1.3	1.7	49.4
H4	—	13 000	1.6	1.8	38.9

[a] Determined *via* ^{1}H NMR analysis. [b] Based on Boc-protected polymers. [c] Determined *via* GPC analysis. [d] Based on Boc-deprotected polymers.

Table 2 Antimicrobial and hemolytic activities of antimicrobial ternary copolymers

	MIC[a] (μg mL^{-1})			HC_{50} (μg mL^{-1})	Selectivity[b]
Entry	*P. aeruginosa*	*E. coli*	*V. cholerae*	RBC	HC_{50}/MIC
L1	32–64	32–64	128	2500	39
L2	64	64	—	>10 000 (major)[c]	—
L3	128	64	—	>10 000 (major)[c]	—
B1	>256	>256	—	—	—
B2	>256	>256	—	—	—
H1	64	32–64	128	>10 000 (minor)[c]	—
H2	64	64	128	>10 000	>156
H3	>256	—	—	—	—
H4	>256	—	—	—	—

[a] The strains are *P. aeruginosa* PAO1, *E. coli* K12, and *V. cholerae* SIO. [b] Selectivity is defined as the ratio of HC_{50} to the MIC against *P. aeruginosa*. [c] Major or minor hemagglutination was observed for these samples. The symbol '—' indicates not determined.

and *Escherichia coli* by determining their MICs (Table 2). As mentioned previously, our focus in this study is on Gram-negative pathogens as infections caused by these bacteria are more severe than those caused by Gram-positive bacteria. L1, L2 and L3 have a similar MIC (64 μg mL^{-1}) against *E. coli*. However, when tested against *P. aeruginosa*, L1 and L2, which have DP_n of 100 and 50, respectively, were slightly more active than L3. This suggests that polymers with the longer chain length are marginally more bacteriostatic than those with shorter chain lengths against *P. aeruginosa*.

Next, we determined the hemocompatibility of L1, L2 and L3 with sheep red blood cells (RBCs) by comparing their HC_{50} values (Table 2). Polymer L1 was more hemolytic than L2 and L3. L1 has a HC_{50} value of 2500 μg mL^{-1} whereas both L2 and L3 resulted in less than 50% lysis of RBCs even when tested at the highest concentration of 10 000 μg mL^{-1}. It is worth noting that the highest polymer concentration used for hemolysis experiments in our previous publication was 2000 μg mL^{-1}.[47] At first glance, L2 and L3 represent polymers with the most optimal biological performance purely based on their MICs and HC_{50} values. However, L2 and L3 caused hemagglutination, as evidenced by the inability to resuspend the RBCs following incubation with the polymers (Movie S1, ESI†). While a high HC_{50} value is indicative of good hemocompatibility, it is also imperative for a compound to exhibit non- or low-hemagglutination for clinical applications. Thus, L2 and L3 cannot be considered as better than L1 in terms of the overall biological performance.

Judging from the combined analysis of MICs and HC_{50} values of L1, L2 and L3, we deduced that the ability of linear random copolymers to cause membrane disruption is possibly influenced by the chain length. It is important to note that the ternary random copolymers were shown to cause membrane wall disruption.[47] The results here seem to indicate that longer polymer chains are (slightly) more effective in lysing membrane cell walls (bacteria or erythrocytes) given that L1 has a lower MIC and HC_{50} than L2 and L3. We postulate that longer polymer chains exhibit more extensive interactions with cell membranes and thus are better at causing membrane disruption events than shorter polymer chains. We are unsure, however, as to why hemagglutination only occurred with shorter polymer chains.

Block copolymer architecture

For the synthesis of block copolymers, a macroRAFT agent was first prepared *via* the random copolymerization of OEG acrylate and *tert*-butyl (4-acrylamidobutyl) carbamate, where the molar ratio of OEG : cationic monomer was set at 1 : 3. The polymerization proceeded at 70 °C for 3 h. The monomer conversion was 80% while the DP_n was *ca.* 50 repeat units as determined by ^{1}H NMR analysis (Fig. S4, ESI†). GPC analysis revealed a monomodal molecular weight distribution with a $Đ$ of 1.4 (Fig. 3a and Table 1).

Two hydrophobic monomers, including 2-ethylhexyl acrylate and 2-phenylethyl acrylate, were subsequently employed in the chain extension steps to yield Boc-protected block copolymers B1 and B2, respectively. ^{1}H NMR analysis revealed that there were *ca.* 30 repeating units of the hydrophobic moieties per chain in B1 and B2 (Fig. S5 and S6, ESI†). Successful chain extension was obtained as the molecular weight distributions of Boc-protected B1 and B2 shifted to shorter retention times, as observed by GPC analysis (Fig. 3a). Following the removal of

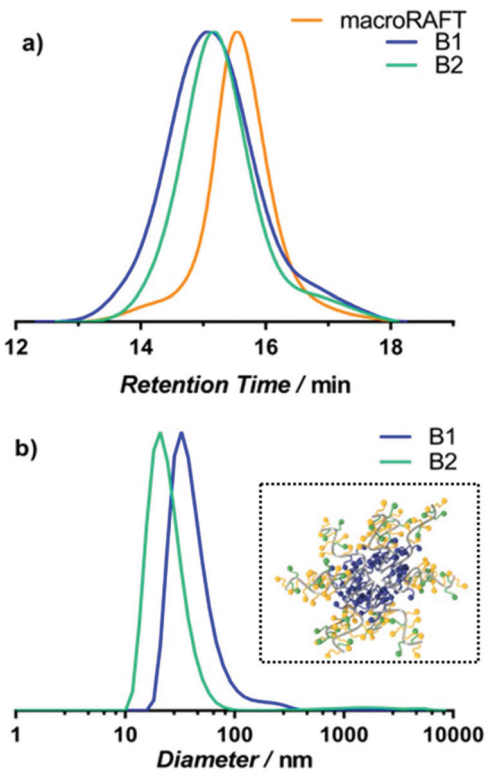

Fig. 3 (a) GPC DRI chromatograms of the macroRAFT agent and Boc-protected polymers B1 and B2. (b) DLS normalized volume distributions of Boc-deprotected B1 and B2 polymers in water. The inset illustrates the formation of micelles *via* the self-assembly of the block copolymers in water.

Boc groups, the self-assembly of the block copolymers in water was followed by DLS. It is worth noting that the molar ratio of the hydrophobic : hydrophilic component was increased from 1 : 4 in the random copolymer system to 3 : 5 in this case to ensure micelle formation in aqueous medium. Micelle formation was evident as DLS analysis revealed peaks with D_h values of 43.7 and 24.6 nm for B1 and B2, respectively (Fig. 3b). Zeta-potential (ζ) analysis also confirmed the cationic character of the micelles, with B1 and B2 registering ζ values of +36.3 and +28.6 mV, respectively. The MICs of micelles B1 and B2 were assessed against *P. aeruginosa* and *E. coli*. To our surprise, B1 and B2 did not display bacteriostatic activity against both the Gram-negative bacteria even at a polymer concentration of 256 μg mL^{-1}. Our initial hypothesis was that the micelles will first establish interactions with the bacterial cell membrane, followed by micelle disassembly and integration into the membrane lipid bilayer to cause membrane disruption. However, the *in vitro* antimicrobial tests suggest that micelles B1 and B2 perhaps never underwent micelle disassembly upon contact with the bacterial cells. Instead, we postulate that the micelles preferentially remain in their core–shell morphology rather than integrating with the bacterial membrane lipid bilayer. It is noteworthy that there are contrasting reports in the literature which suggest that block copolymers may or may not possess inherent antimicrobial activity.[43] We strongly believe that the antimicrobial properties of block copolymers vary across systems (*e.g.*, different polymer backbones, monomer combinations and types) and specifically in our case, the block copolymers are inactive against Gram-negative bacteria. Given that B1 and B2 were inactive against the bacteria, we did not pursue further hemolysis experiments with these polymers.

Hyperbranched architecture

The synthesis of hyperbranched polymers was performed in the same fashion as for the linear random copolymers, albeit with the addition of a cross-linkable monomer (OEG diacrylate), similar to literature procedures.[49–56] Two hyperbranched polymers which consisted of 2-ethylhexyl groups as the hydrophobic component, labelled as H1 and H2, were prepared using 2 and 5 molar equivalents of OEG diacrylate to the RAFT initiator, respectively. For both polymers, the polymerization was taken to full monomer conversion, as confirmed by ^{1}H NMR analysis (Fig. S7 and S8, ESI†). GPC analysis of the Boc-protected H1 and H2 revealed multimodal molecular weight distributions typically observed for hyperbranched polymers,[51] with H2 having a broader distribution and higher molecular weight species than H1 (Fig. 4a). After the removal of Boc groups, DLS analysis of the hyperbranched polymers showed that H1 and H2 have D_h values of 1.7 and 1.6 nm, respectively (Fig. 4b and Table 1). Meanwhile, the zeta potential measurement confirmed the cationic nature of the polymers (ζ > 36 mV). It is worth noting that the zeta potential and hydrodynamic volume of the hyperbranched and linear random copolymers are comparable.

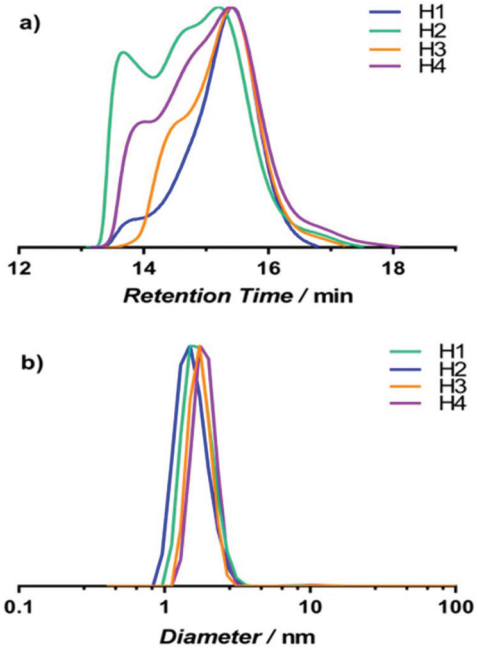

Fig. 4 (a) GPC DRI chromatograms of the Boc-protected hyperbranched polymers H1, H2, H3 and H4. (b) DLS normalized volume distributions of Boc-deprotected H1, H2, H3 and H4 polymers in water.

The MIC of H1 and H2 against *P. aeruginosa* and *E. coli* was 64 μg mL^{-1}, which was similar to the linear random copolymers L1 and L2. In terms of hemocompatibility, both H1 and H2 have an HC_{50} value of >10 000 μg mL^{-1}, but H1 caused minor hemagglutination whereas H2 did not (Movie S2, ESI†). Polymers prepared with a higher amount of OEG diacrylate prevented hemagglutination from occurring. This is especially true considering that major hemagglutination was present in L2. The experiments involving RBCs thus strongly suggest that branching in polymer structures can reduce the occurrence of hemagglutination, though the mechanism is unclear. We also prepared two additional hyperbranched polymers H3 and H4 that were made in the exact same manner as H1 and H2, respectively, but with 2-phenylethyl groups as the hydrophobic component. Surprisingly, H3 and H4 were inactive against the bacteria tested, even at a higher polymer concentration of 256 μg mL^{-1}. This suggests that the ethylhexyl groups in branched polymers have better membrane disruption capabilities compared to phenylethyl groups, thereby leading to higher antimicrobial activity.

Taken together, hyperbranched polymer H2 has the best overall biological performance in this study. H2 has a selectivity (defined here as the ratio of HC_{50} to MIC against *P. aeruginosa*) of >156, which is >4 times greater than the selectivity of L1, one of the two lead polymers in our previous study.[47] Further tests were performed with H2 (and H1) to ascertain their antimicrobial potency. H1 and H2 were tested against a highly pathogenic Gram-negative species, *Vibrio cholerae*. The obtained MIC was 128 μg mL^{-1} which was the same as L1, thus confirming the ability of H1 and H2 in combating

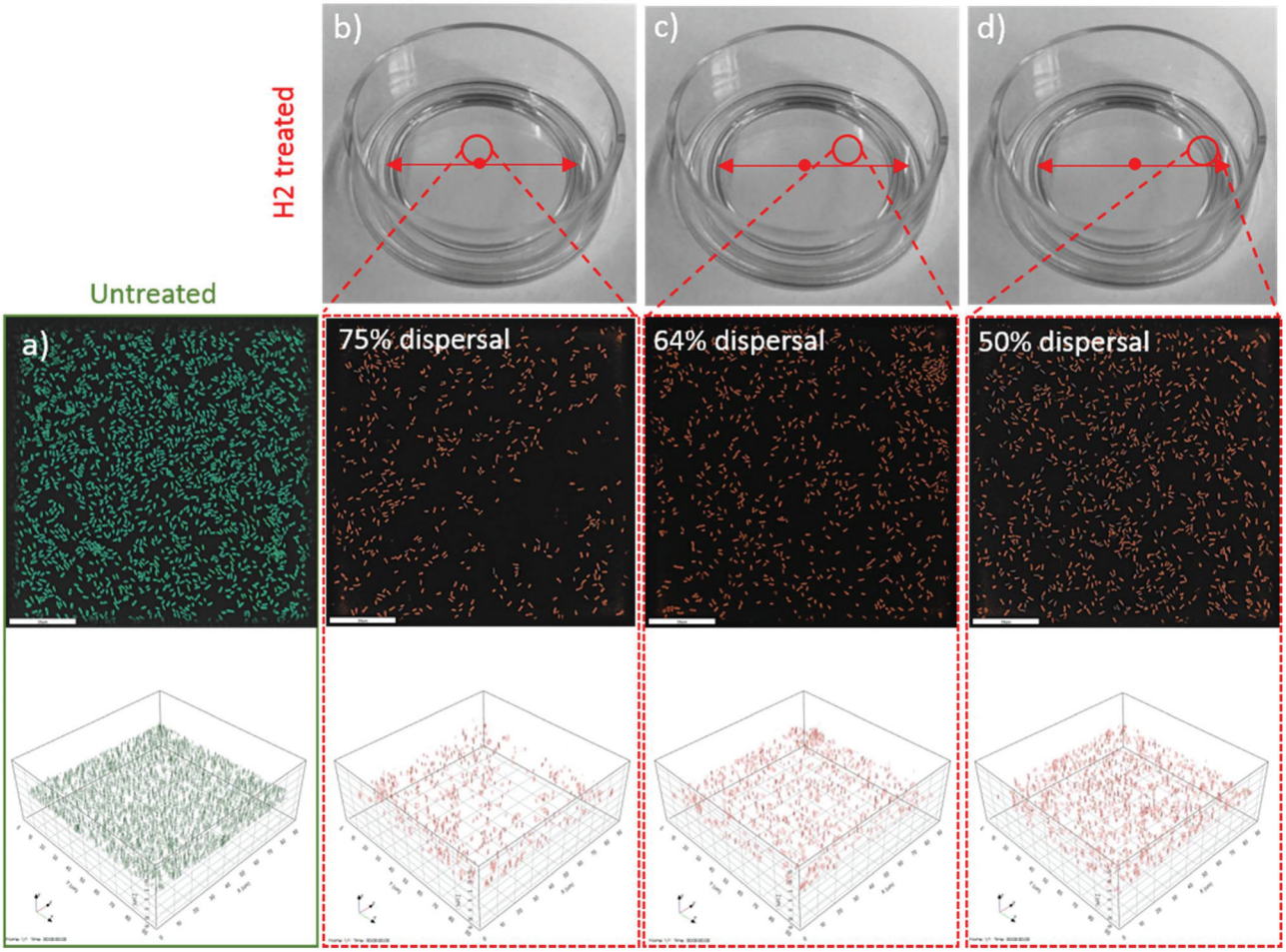

Fig. 5 2D and 3D tomographic microscopy images of the untreated control (a) and H2 treated samples (b–d). Scale bar = 20 μm.

more pathogenic bacteria strains. Next, we investigated the ability of H2 to combat biofilms. Biofilm-related infections are usually hard to treat and often the main cause of chronic inflammation. For this experiment, *P. aeruginosa* biofilms were grown in the M9 medium for 6.5 h prior to incubation with the polymer for 1 h. Based on colony-forming unit (CFU) analysis, H2 (at a dosage of 64 μg mL^{-1}) demonstrated good bactericidal properties, killing ≥99% and 90% of planktonic and biofilm bacteria, respectively. In addition, H2 was also capable of dispersing preformed biofilms. The treatment of *P. aeruginosa* biofilms with 64 μg mL^{-1} of H2 for 1 h resulted in 46% reduction in biofilm biomass compared to untreated controls, as determined by the crystal violet (CV) staining assay. The biofilm biomass that remained following dispersal events was also visualized using a 3D tomographic microscope (NanoLive) with digital staining software (Fig. 5). Interestingly, it was observed that there was less biofilm in the centre of the well compared to the edges in the H2 treated samples. Approximately, 63% of biofilm biomass was reduced (compared to untreated controls) taking into account the average of these different areas. For the untreated controls, the density of the biofilm was identical throughout the well. It is noteworthy that although the biofilm dispersal induced by H2 was not uniform, the majority (90%) of the remaining biofilm biomass are dead bacteria according to the CFU analysis.

Conclusions

In summary, a series of amphiphilic ternary copolymers composed of oligoethylene glycol, cationic and hydrophobic functional groups, and with different chain lengths and topologies were synthesized and evaluated for their antimicrobial efficacy and hemocompatibility. Gram-negative bacteria such as *P. aeruginosa* and *E. coli* were used to determine the antimicrobial activity of the polymers. The chain length of linear random copolymers has little influence on the antimicrobial activity, with longer chains having slightly higher antimicrobial activity. However, we found that shorter polymer chains cause hemagglutination. When the hydrophilic and hydrophobic segments were segregated into two distinct blocks, the block copolymers lost their antimicrobial activity. Importantly, hyperbranched random copolymers that contain 2-ethylhexyl groups were observed to have the best overall bio-

logical performance, with HC_{50} > 10 000 μg mL^{-1}, no hemagglutination, and an MIC of 64 μg mL^{-1} against *P. aeruginosa* and *E. coli*. Although hyperbranched random copolymers have slightly lower antimicrobial activity than linear random copolymers, the branched structures have higher hemocompatibility (by >4 times). The hyperbranched polymers were also capable of killing planktonic and biofilm bacteria, as well as inducing the dispersal of biofilms. Taken together, this study thus helps in identifying key macromolecular variations that will aid in the design of bio- and hemo-compatible antimicrobial polymers.

Conflicts of interest

There are no conflicts of interest to declare.

Acknowledgements

This work was supported by UNSW Australia and the Australian Research Council *via* the 2016 UNSW Vice-Chancellor's Research Fellowship (E. H. H. W.) and Future Fellowship (FT120100096, C. B.), respectively. We acknowledge the facilities and technical assistance provided by the Mark Wainwright Analytical Centre at UNSW Australia *via* the Nuclear Magnetic Resonance Facility (Dr Donald Thomas and Dr Adelle Amore). We also acknowledge some of the facilities provided by the Centre for Marine Bio-Innovation at UNSW. S. H. O. acknowledges the receipt of NHMRC funding in the form of Project Grant (1099912) and CJ Martin Early Career Fellowship (1053407).

Notes and references

1 G. D. Wright, *ACS Infect. Dis.*, 2015, **1**, 80–84.
2 G. Taubes, *Science*, 2008, **321**, 356–361.
3 Y. Wo, E. J. Brisbois, R. H. Bartlett and M. E. Meyerhoff, *Biomater. Sci.*, 2016, **4**, 1161–1183.
4 J. Song and J. Jang, *Adv. Colloid Interface Sci.*, 2014, **203**, 37–50.
5 C. Willyard, *Nature*, 2017, **543**, DOI: 10.1038/nature.2017.21550.
6 L. L. Ling, T. Schneider, A. J. Peoples, A. L. Spoering, I. Engels, B. P. Conlon, A. Mueller, T. F. Schäberle, D. E. Hughes, S. Epstein, M. Jones, L. Lazarides, V. A. Steadman, D. R. Cohen, C. R. Felix, K. A. Fetterman, W. P. Millett, A. G. Nitti, A. M. Zullo, C. Chen and K. Lewis, *Nature*, 2015, **517**, 455–459.
7 D. J. Payne, M. N. Gwynn, D. J. Holmes and D. L. Pompliano, *Nat. Rev. Drug Discovery*, 2007, **6**, 29–40.
8 C. Boyer, V. Bulmus, T. P. Davis, V. Ladmiral, J. Liu and S. Perrier, *Chem. Rev.*, 2009, **109**, 5402–5436.
9 C. J. Hawker, A. W. Bosman and E. Harth, *Chem. Rev.*, 2001, **101**, 3661–3688.
10 K. Matyjaszewski and J. Xia, *Chem. Rev.*, 2001, **101**, 2921–2990.
11 K. Matyjaszewski and N. V. Tsarevsky, *Nat. Chem.*, 2009, **1**, 276–288.
12 G. Moad, E. Rizzardo and S. H. Thang, *Aust. J. Chem.*, 2009, **62**, 1402–1472.
13 G. Moad, E. Rizzardo and S. H. Thang, *Chem. – Asian J.*, 2013, **8**, 1634–1644.
14 K. Kuroda, G. A. Caputo and W. F. DeGrado, *Chem. – Eur. J.*, 2009, **15**, 1123–1133.
15 M. F. Ilker, K. Nüsslein, G. N. Tew and E. B. Coughlin, *J. Am. Chem. Soc.*, 2004, **126**, 15870–15875.
16 K. Kuroda and W. F. DeGrado, *J. Am. Chem. Soc.*, 2005, **127**, 4128–4129.
17 Y. Ishitsuka, L. Arnt, J. Majewski, S. L. Frey, M. Ratajczak, K. Kjaer, G. N. Tew and K. Y. C. Lee, *J. Am. Chem. Soc.*, 2008, **130**, 2372–2372.
18 E. F. Palermo, I. Sovadinova and K. Kuroda, *Biomacromolecules*, 2009, **10**, 3098–3107.
19 E. F. Palermo, S. Vemparala and K. Kuroda, *Biomacromolecules*, 2012, **13**, 1632–1641.
20 L. C. Paslay, B. A. Abel, T. D. Brown, V. Koul, V. Choudhary, C. L. McCormick and S. E. Morgan, *Biomacromolecules*, 2012, **13**, 2472–2482.
21 T. D. Michl, K. E. Locock, N. E. Stevens, J. D. Hayball, K. Vasilev, A. Postma, Y. Qu, A. Traven, M. Haeussler and L. Meagher, *Polym. Chem.*, 2014, **5**, 5813–5822.
22 B. P. Mowery, A. H. Lindner, B. Weisblum, S. S. Stahl and S. H. Gellman, *J. Am. Chem. Soc.*, 2009, **131**, 9735–9745.
23 H. Wang, X. Shi, D. Yu, J. Zhang, G. Yang, Y. Cui, K. Sun, J. Wang and H. Yan, *Langmuir*, 2015, **31**, 13469–13477.
24 A. Punia, A. Mancuso, P. Banerjee and N.-L. Yang, *ACS Macro Lett.*, 2015, **4**, 426–430.
25 J. Zhang, M. J. Markiewicz, B. P. Mowery, B. Weisblum, S. S. Stahl and S. H. Gellman, *Biomacromolecules*, 2012, **13**, 323–331.
26 Y. Oda, S. Kanaoka, T. Sato, S. Aoshima and K. Kuroda, *Biomacromolecules*, 2011, **12**, 3581–3591.
27 Y. Wang, J. Xu, Y. Zhang, H. Yan and K. Liu, *Macromol. Biosci.*, 2011, **11**, 1499–1504.
28 G. N. Tew, R. W. Scott, M. L. Klein and W. F. DeGrado, *Acc. Chem. Res.*, 2009, **43**, 30–39.
29 K. Lienkamp and G. N. Tew, *Chem. – Eur. J.*, 2009, **15**, 11784–11800.
30 K. Lienkamp, A. E. Madkour, K. N. Kumar, K. Nüsslein and G. N. Tew, *Chem. – Eur. J.*, 2009, **15**, 11715–11722.
31 K. Lienkamp, K. N. Kumar, A. Som, K. Nüsslein and G. N. Tew, *Chem. – Eur. J.*, 2009, **15**, 11710–11714.
32 H. Takahashi, G. A. Caputo, S. Vemparala and K. Kuroda, *Bioconjugate Chem.*, 2017, **28**, 1340–1350.
33 M. Porel, D. N. Thornlow, N. N. Phan and C. A. Alabi, *Nat. Chem.*, 2016, **8**, 590–596.
34 M. Zasloff, *Nature*, 2002, **415**, 389–395.
35 S. J. Lam, E. H. H. Wong, N. M. O'Brien-Simpson, N. Pantarat, A. Blencowe, E. C. Reynolds and G. G. Qiao, *ACS Appl. Mater. Interfaces*, 2016, **8**, 33446–33456.
36 S. J. Lam, N. M. O'Brien-Simpson, N. Pantarat, A. Sulistio, E. H. H. Wong, Y.-Y. Chen, J. C. Lenzo, J. A. Holden, A. Blencowe, E. C. Reynolds and G. G. Qiao, *Nat. Microbiol.*, 2016, **1**, 16162.

37 E.-R. Kenawy, S. D. Worley and R. Broughton, *Biomacromolecules*, 2007, **8**, 1359–1383.
38 E. F. Palermo and K. Kuroda, *Biomacromolecules*, 2009, **10**, 1416–1428.
39 M. Mizutani, E. F. Palermo, L. M. Thoma, K. Satoh, M. Kamigaito and K. Kuroda, *Biomacromolecules*, 2012, **13**, 1554–1563.
40 W. Yuan, J. Wei, H. Lu, L. Fan and J. Du, *Chem. Commun.*, 2012, **48**, 6857–6859.
41 E. H. Wong, M. M. Khin, V. Ravikumar, Z. Si, S. A. Rice and M. B. Chan-Park, *Biomacromolecules*, 2016, **17**, 1170–1178.
42 X. Wan, Y. Zhang, Y. Deng, Q. Zhang, J. Li, K. Wang, J. Li, H. Tan and Q. Fu, *Soft Matter*, 2015, **11**, 4197–4207.
43 S. J. Lam, E. H. H. Wong, C. Boyer and G. G. Qiao, *Prog. Polym. Sci.*, 2017, DOI: 10.1016/j.progpolymsci.2017.07.007.
44 X. Chen, G. Zhang, Q. Zhang, X. Zhan and F. Chen, *Ind. Eng. Chem. Res.*, 2015, **54**, 3813–3820.
45 G. Cheng, H. Xue, G. Li and S. Jiang, *Langmuir*, 2010, **26**, 10425–10428.
46 L. Mi and S. Jiang, *Biomaterials*, 2012, **33**, 8928–8933.
47 T.-K. Nguyen, S. J. Lam, K. K. Ho, N. Kumar, G. G. Qiao, S. Egan, C. Boyer and E. H. H. Wong, *ACS Infect. Dis.*, 2017, **3**, 237–248.
48 S. P. Liu, L. Zhou, R. Lakshminarayanan and R. W. Beuerman, *Int. J. Pept. Res. Ther.*, 2010, **16**, 199–213.
49 M. Luzon, C. Boyer, C. Peinado, T. Corrales, M. Whittaker, L. Tao and T. P. Davis, *J. Polym. Sci., Part A: Polym. Chem.*, 2010, **48**, 2783–2792.
50 N. O'Brien, A. McKee, D. C. Sherrington, A. T. Slark and A. Titterton, *Polymer*, 2000, **41**, 6027–6031.
51 H. Gao and K. Matyjaszewski, *Prog. Polym. Sci.*, 2009, **34**, 317–350.
52 A. T. Slark, D. C. Sherrington, A. Titterton and I. K. Martin, *J. Mater. Chem.*, 2003, **13**, 2711–2720.
53 A. P. Vogt and B. S. Sumerlin, *Macromolecules*, 2008, **41**, 7368–7373.
54 F. Isaure, P. A. G. Cormack and D. C. Sherrington, *J. Mater. Chem.*, 2003, **13**, 2701–2710.
55 Z. Wang, J. He, Y. Tao, L. Yang, H. Jiang and Y. Yang, *Macromolecules*, 2003, **36**, 7446–7452.
56 C. Li, J. He, L. Li, J. Cao and Y. Yang, *Macromolecules*, 1999, **32**, 7012–7014.